

Electron-phonon coupling in crystalline organic semiconductors: Microscopic evidence for nonpolaronic charge carriers

Nenad Vukmirović,^{1,*} C. Bruder,² and Vladimir M. Stojanović^{2,†}

¹*Scientific Computing Laboratory, Institute of Physics Belgrade,
University of Belgrade, Pregrevica 118, 11080 Belgrade, Serbia*

²*Department of Physics, University of Basel, Klingelbergstrasse 82, CH-4056 Basel, Switzerland
(Dated: May 30, 2018)*

We consider electron(hole)-phonon coupling in crystalline organic semiconductors, using naphthalene for our case study. Employing a first-principles approach, we compute the changes in the self-consistent Kohn-Sham potential corresponding to different phonon modes and go on to obtain the carrier-phonon coupling matrix elements (vertex functions). We then evaluate perturbatively the quasiparticle spectral residues for electrons at the bottom of the lowest-unoccupied- (LUMO) and holes at the top of the highest-occupied (HOMO) band, respectively obtaining $Z_e \approx 0.74$ and $Z_h \approx 0.78$. Along with the widely accepted notion that the carrier-phonon coupling strengths in polyacenes decrease with increasing molecular size, our results provide a strong microscopic evidence for the previously conjectured nonpolaronic nature of band-like carriers in these systems.

PACS numbers: 71.38.-k, 72.80.Le, 78.55.Kz

High-purity crystalline organic semiconductors, best exemplified by polyacenes, have attracted a great deal of interest as they hold promise for plastic electronics [1, 2]. Despite many theoretical [3–8] and experimental [9–11] studies, a controversy persists regarding the nature of charge carriers in these π -electron systems with weak van der Waals intermolecular interactions. Are these carriers of polaronic character or not? Elucidating this important issue would pave the way for understanding the intrinsic (bulk) charge transport in polyacenes and transport in the organic field-effect-transistor geometry [10]. While recent theoretical studies have provided a qualitative case for non-polaronic carriers [12, 13], this conclusion has yet to be borne out through a detailed microscopic analysis of the underlying electron(hole)-phonon (e-ph) coupling.

While the e-ph coupling in inorganic semiconductors is rather weak, in their narrow-band organic counterparts (the conduction- and valence bandwidths in polyacenes are $W \sim 0.1 - 0.4$ eV) it plays a prominent role [14, 15]. Like in other π -electron systems, this interaction has a strong momentum dependence stemming from Peierls' coupling mechanism [16, 17], whereby lattice displacements affect electronic hopping integrals. Given their structural complexity and pronounced anisotropy, e-ph coupling in organic semiconductors is typically described using tight-binding-type models, for simplicity often taken to be one-dimensional and merely involving Einstein phonons. Although such simplified models often lead to qualitatively correct results, they cannot be considered quantitatively reliable as even the bare band structure of polyacenes can only be accurately reproduced if at least three different hopping integrals are taken into account [18].

In this Letter, on the example of the naphthalene crystal [see Fig. 1(a)], we systematically investigate e-ph coupling in organic semiconductors. As a by-product of

an electronic-structure calculation performed within the density functional theory (DFT) framework, we compute the changes in the self-consistent Kohn-Sham potential for electrons in the LUMO- and holes in the HOMO band coupled to different optical phonon modes. By sampling the e-ph scattering processes throughout the Brillouin zone (BZ) [Fig. 1(b)], we extract the corresponding (momentum-dependent) coupling matrix elements [19] and make use of the latter to perturbatively compute the quasiparticle spectral residues and inelastic scattering rates. In particular, the values we obtain for the quasiparticle residues of electrons at the bottom of the LUMO band ($Z_e \approx 0.74$) and holes at the top of the HOMO band ($Z_h \approx 0.78$) indicate that the band-like carriers in naphthalene do not have polaronic character. This conclusion can be carried over to higher polyacenes (anthracene, tetracene, pentacene) in which e-ph coupling becomes progressively weaker.

We make use of the Quantum-ESPRESSO [20] code, with

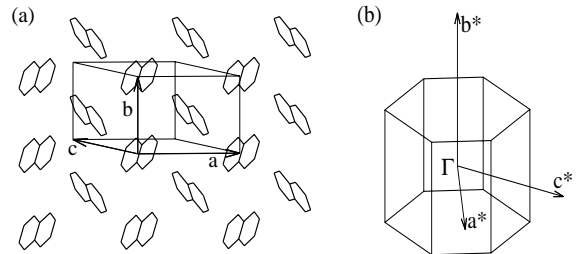


FIG. 1: (a) An illustration of the crystal structure of naphthalene, comprising molecular layers (in the $a - b$ plane) stacked in the crystallographic c direction. Each unit cell contains two inequivalent naphthalene molecules in a herringbone-like arrangement. (b) The irreducible wedge of the Brillouin zone in the naphthalene crystal. The zone center (Γ -point) is indicated, along with the reciprocal basis vectors.

the core-valence interaction taken into account through a norm-conserving pseudopotential with kinetic energy cutoff of 60 Ry. Our first-principles scheme employs the PBE GGA exchange-correlation functional with semiempirical correction for van der Waals interaction [21]. The functionals specifically tailored for this type of weak intermolecular interaction have proven to yield accurate cohesive energies of polyacenes [22]. Our calculations of the phonon spectrum and e-ph matrix elements are based on density-functional perturbation theory [23].

The momentum-space form of the most general (multi-band) e-ph-coupling Hamiltonian reads

$$\hat{H}_{\text{e-ph}} = \frac{1}{\sqrt{N}} \sum_{nn', \mathbf{k}, \mathbf{q}, \lambda} \gamma_{n'n}^{\lambda}(\mathbf{k}, \mathbf{q}) \hat{a}_{n', \mathbf{k}+\mathbf{q}}^{\dagger} \hat{a}_{n, \mathbf{k}} (\hat{b}_{-\mathbf{q}, \lambda}^{\dagger} + \hat{b}_{\mathbf{q}, \lambda}), \quad (1)$$

where $\hat{a}_{n, \mathbf{k}}$ destroys an electron with quasimomentum \mathbf{k} in the n -th Bloch band, $\hat{b}_{\mathbf{q}, \lambda}$ a phonon of branch λ with quasimomentum \mathbf{q} (frequency $\omega_{\lambda, \mathbf{q}}$), and

$$\gamma_{n'n}^{\lambda}(\mathbf{k}, \mathbf{q}) = \sqrt{\frac{\hbar}{2\omega_{\lambda, \mathbf{q}}}} \sum_{S\alpha} e_{S\alpha}^{(\lambda)}(\mathbf{q}) \frac{1}{\sqrt{M_S}} \times \left\langle \psi_{n', \mathbf{k}+\mathbf{q}} \left| \frac{\partial U_{\text{scf}}}{\partial u_{\mathbf{q}S\alpha}} \right| \psi_{n, \mathbf{k}} \right\rangle \quad (2)$$

stand for the (bare) e-ph interaction vertex functions. In the last expression, $|\psi_{n\mathbf{k}}\rangle$ and $|\psi_{n', \mathbf{k}+\mathbf{q}}\rangle$ are electronic Bloch states, U_{scf} is the self-consistent Kohn-Sham potential, $e_{S\alpha}^{(\lambda)}(\mathbf{q})$ is the component of the eigenvector of the dynamical matrix $D(\mathbf{q})$ corresponding to the displacement of the S -th atom (mass M_S) in direction α due to the phonon mode (λ, \mathbf{q}) , while $u_{\mathbf{q}S\alpha} \equiv N^{-1} \sum_p \exp(i\mathbf{q} \cdot \mathbf{R}_p) u_{pS\alpha}$, where \mathbf{R}_p ($p = 1, \dots, N$) denotes unit cells and $u_{pS\alpha}$ the displacement of the atom S from unit cell p in direction α .

The crux of our treatment is a first-principles evaluation of the vertex functions in Eq. (2) for two pairs of HOMO- and LUMO-derived bands, respectively denoted by (HOMO-1, HOMO), and (LUMO, LUMO+1). These functions incorporate the contributions of the corresponding phonon modes to all the existing e-ph coupling mechanisms. The actual momentum dependence that characterizes the coupling to a given phonon mode depends in a complex way on the underlying molecular-crystal geometry, the symmetry of the mode involved, as well as the spatial directionality of the π -electron orbitals [26]. Such aspects clearly cannot be accounted for within simplified (low-dimensional) tight-binding-type models, hence providing a rationale for our rigorous – albeit computationally much more demanding – approach.

The electronic structure and phonon spectra calculations were performed on a uniform $6 \times 6 \times 6$ momentum grid. The changes of U_{scf} with respect to atomic-displacement perturbations were obtained using the `Phonon` code from the `Quantum-ESPRESSO` [20] package, while the matrix elements in Eq. (2) were extracted

from the `EPW` code [24]. Our own implementation of the Fourier-Wannier interpolation scheme for e-ph matrix elements [19] was then used to obtain the matrix elements on a dense $24 \times 24 \times 24$ grid, which is necessary for achieving high accuracy when computing \mathbf{q} -space integrals. The `Wannier90` code [25] was employed to get the maximally-localized Wannier functions needed for this interpolation scheme. While this methodology has heretofore been used for systems with few atoms per unit cell [19], our implementation enabled its application to a system with as many as 36 atoms.

We computed the e-ph vertex functions for different phonon branches λ and quasimomenta \mathbf{k} , \mathbf{q} throughout the BZ. The strong momentum dependence and the anisotropic character of these functions, especially in the $a - b$ plane, is illustrated in Fig. 2 for electrons at the bottom of the LUMO band ($\mathbf{k} = 0$) and holes at the top of the HOMO band ($\mathbf{k} = 0.5 \mathbf{a}^* + 0.5 \mathbf{b}^*$) interacting with the lowest-branch (intermolecular) optical phonons of rotational (librational) origin. This strong momentum dependence serves as evidence for the dominance of the Peierls-type (off-diagonal) e-ph coupling over the strictly local Holstein-type coupling, as the latter yields completely momentum-independent vertex functions. Besides, contrary to what is often assumed in the literature, our calculations show that the coupling to the high-energy intramolecular phonon modes is not necessarily much weaker than the coupling to the intermolecular ones. Among the intramolecular branches the

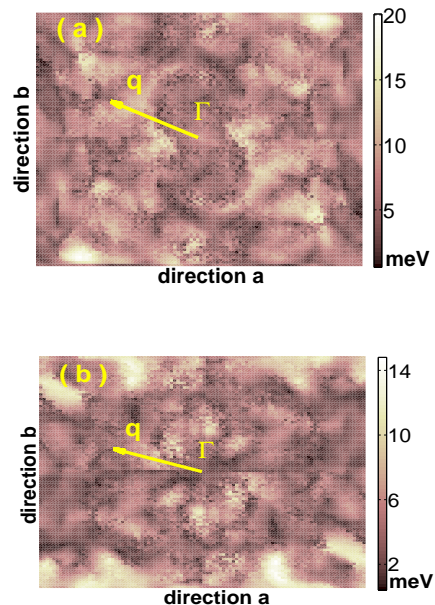


FIG. 2: Calculated phonon-momentum dependence of the moduli of the e-ph vertex functions in the $a - b$ plane for (a) electrons at the bottom of the LUMO band, and (b) holes at the top of the HOMO band, interacting with phonons of the lowest optical branch (the zone-center energy is 11.4 meV).

most relevant ones are two pairs with the respective zone-center energies of approximately 172 meV and 194 meV.

The renormalization due to e-ph coupling is characterized by the quasiparticle spectral residue $Z_n(\mathbf{k}) \equiv |\langle \Psi_{n\mathbf{k}} | \psi_{n\mathbf{k}} \rangle|^2$, where $|\psi_{n\mathbf{k}}\rangle$ is a bare-electron (or hole) state in the n -th Bloch band and $|\Psi_{n\mathbf{k}}\rangle$ that of the coupled e-ph system. Our calculations show that the average values of the momentum-dependent vertex functions (over all the phonon branches and quasimomenta) are approximately 6.8 meV for the HOMO-band holes and 7.8 meV for the LUMO-band electrons. These average values, i.e., their relative smallness compared to the HOMO- and LUMO bandwidths (234.3 and 207.6 meV, respectively), justify a perturbative evaluation of the quasiparticle residues. Within the framework of Rayleigh-Schrödinger (RS) perturbation theory, in the lowest nonvanishing (second) order one obtains

$$Z_n^{-1}(\mathbf{k}) = 1 + \frac{1}{N} \sum_{n', \mathbf{q}, \lambda} \frac{|\gamma_{n'n}^\lambda(\mathbf{k}, \mathbf{q})|^2}{[\varepsilon_n(\mathbf{k}) - \varepsilon_{n'}(\mathbf{k} + \mathbf{q}) - \hbar\omega_{\lambda, \mathbf{q}}]^2}, \quad (3)$$

where $\varepsilon_n(\mathbf{k})$ is the band dispersion.

Given the pairs of energetically close HOMO- and LUMO-derived bands, for electrons at the bottom of the LUMO band the interband contributions [the terms with $n' \neq n$ in Eq. (3)] originate from the LUMO+1 band, while for holes at the top of the HOMO band such contributions stem from its HOMO-1 counterpart. We obtain $Z_e \approx 0.74$ and $Z_h \approx 0.78$ for the quasiparticle residues of electrons and holes, respectively. The contributions of different phonon modes to the quasiparticle renormalization are shown in Fig. 3, which illustrates the prominent role of high-energy intramolecular phonons for both electrons and holes. From RS perturbation the-

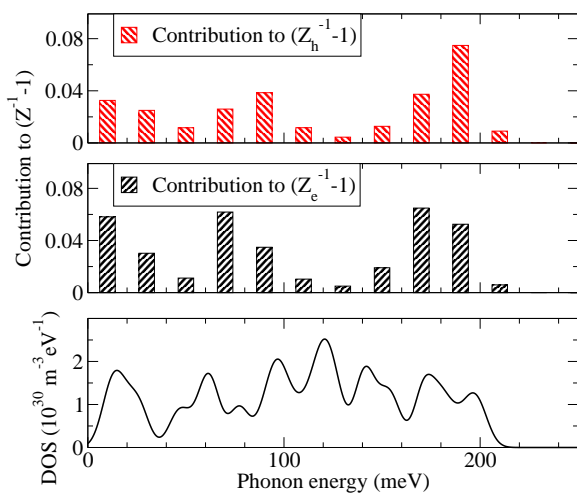


FIG. 3: Upper panel: Contributions of different phonon modes, divided into 20 meV-wide energy intervals, to the quasiparticle renormalization for electrons and holes. Lower panel: Phonon density-of-states (DOS).

ory, we also find the carrier binding (relaxation) energies: $E_b = 68.7$ meV (58.8 meV) for electrons (holes).

To check whether the e-ph coupling in the system is weak enough for second-order RS perturbation theory to be reliable, we also computed Z_e using the self-consistent Born approximation (SCBA). The SCBA self-energy is based on all second-order diagrams and an infinite (non-crossing) subset of higher-order ones [26]. Given that the SCBA approach is computationally extremely demanding, the calculation was done using the original $6 \times 6 \times 6$ grid and taking only the LUMO band into account. The obtained result $Z_e \approx 0.78$ agrees rather well with the RS result obtained on the same grid and with only intraband processes taken into account ($Z_e \approx 0.77$, slightly larger than $Z_e \approx 0.74$ obtained on a dense $24 \times 24 \times 24$ grid). The agreement between the two values suggests that we are in the weak-coupling regime where RS perturbation theory is as accurate as more sophisticated approaches.

The fact that $Z_h > Z_e$ indicates that the carrier-phonon coupling is somewhat stronger for electrons than for holes, thus corroborating the conclusions of some earlier studies [14]. Furthermore, the rather large values obtained for Z_e and Z_h suggest that the phonon-induced renormalization is insufficient for these carriers to have polaronic character. While a direct comparison to polaron models with dispersionless phonons is not possible, let us mention that, e.g., in the Holstein model $Z = 0.1 - 0.2$ at the onset of self trapping (the actual value of Z depends on the dimensionality and the ratio of the hopping integral and the relevant phonon energy) [27]. Another argument in favor of non-polaronic carriers comes from the comparison of their binding energies and the half-bandwidths: the criterion for small (lattice) polaron [28] formation $E_b \geq W/2$ is neither satisfied for electrons nor for holes. While our present analysis is restricted to naphthalene, the last conclusion about the non-polaronic nature of carriers can be generalized to higher polyacenes. The e-ph coupling strengths in these systems are known to decrease (while the HOMO- and LUMO bandwidths increase) with increasing molecular size, thus disfavoring polaron formation.

Quite generally, the total inelastic scattering rate (inverse scattering time) for an electron (or a hole) with quasimomentum \mathbf{k} in the n -th Bloch band is given by

$$\left(\frac{1}{\tau}\right)_{n\mathbf{k}} = \frac{2\pi}{N\hbar} \sum_{n', \mathbf{q}, \lambda} |\gamma_{n'n}^\lambda(\mathbf{k}, \mathbf{q})|^2 \left(\Delta_{n'n}^{\lambda,-} + \Delta_{n'n}^{\lambda,+}\right), \quad (4)$$

where both the intraband ($n' = n$) and interband ($n' \neq n$) carrier scattering processes into states with quasimomenta $\mathbf{k} + \mathbf{q}$ are taken into account, and

$$\Delta_{n'n}^{\lambda, \pm} \equiv (n_{\lambda, \mathbf{q}} + 1/2 \pm 1/2) \delta(\varepsilon_{n', \mathbf{k} + \mathbf{q}} - \varepsilon_{n, \mathbf{k}} \pm \hbar\omega_{\lambda, \mathbf{q}}) \quad (5)$$

corresponds to the emission (+) or absorption (-) of a phonon (λ, \mathbf{q}); $n_{\lambda, \mathbf{q}} \equiv [\exp(\hbar\omega_{\lambda, \mathbf{q}}/k_B T) - 1]^{-1}$ are the phonon occupation numbers at temperature T .

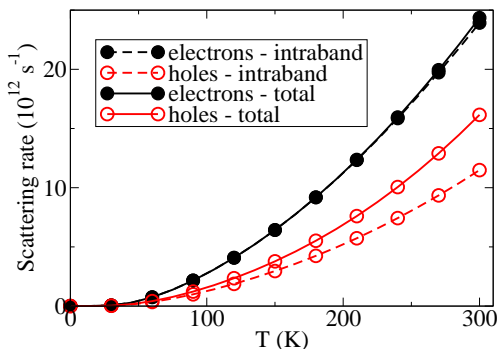


FIG. 4: The temperature dependence of inelastic scattering rates for band-like electron- and hole states in naphthalene.

Based on Eq. (4) and the calculated vertex functions, we evaluate the scattering rates at different temperatures for an electron at the bottom of the LUMO band and a hole at the top of the HOMO band, with the interband contributions originating from LUMO+1 and HOMO-1 bands, respectively. The results, displayed in Fig. 4, show that for electrons the interband-scattering contribution is practically negligible, while for holes it is rather significant. This can be understood by noting that the HOMO and HOMO-1 bands have a large overlap through much of the BZ [18]. Importantly, from Fig. 4 it can be inferred that even at room temperature the values of \hbar/τ for both electrons and holes are sufficiently smaller than the corresponding bandwidths that we can talk about well-defined, weakly renormalized, Bloch states.

Let us now put our results in perspective by clarifying their connection to the existing theories of crystalline organic semiconductors. The long-held consensus that the conventional Bloch-Boltzmann theory is inadequate for describing transport properties of these systems [3], as well as the awareness of the relevance of e-ph interaction, have led workers in the field to adopt polaron models [4–7]. The appeal to such models was partly motivated by the apparent mean free paths of carriers in these systems being even below the intermolecular distance (the Mott-Ioffe-Regel limit). Yet, Troisi *et al.* [12] put forward the idea of a temperature-driven dynamic disorder of these soft materials, which calls into question the applicability of the band concept but nonetheless allows one to reproduce the metallic-like power-law temperature dependence of the charge mobility seen in experiments. The characteristic duality between the band-like and incoherent carrier states was finally explained by Fratini and Ciuchi in their semi-phenomenological model [13]. One of the crucial assumptions underpinning this model is that the band-like states are only weakly renormalized by the interaction with lattice vibrations. This weak renormalization, indicating the absence of polarons, is quantitatively demonstrated by our present microscopic study.

To conclude, on the example of naphthalene we have

studied carrier-phonon coupling in crystalline organic semiconductors. By combining a rigorous first-principles evaluation of coupling matrix elements and a perturbative many-body analysis, we established that the band-like carrier states in these systems do not undergo a sufficiently strong phonon-induced renormalization to have polaronic character. Our study thus provides a useful, up to now unavailable, microscopic insight into the nature of charge carriers in organic molecular crystals.

Useful discussions with F. Giustino are gratefully acknowledged. N.V. was supported by European Community FP7 Marie Curie Career Integration Grant (ELECTROMAT), the Serbian Ministry of Science (project ON171017) and FP7 projects PRACE-1IP, PRACE-2IP, HP-SEE and EGI-InSPIRE. V.M.S. and C.B. were supported by the Swiss NSF and the NCCR Nanoscience.

* Electronic address: nenad.vukmirovic@ipb.ac.rs

† Electronic address: vladimir.stojanovic@unibas.ch

- [1] For an introduction, see N. Karl, in *Organic Electronic Materials* (Springer-Verlag, Berlin, 2001), edited by R. Farchioni and G. Grosso, pp. 283-326.
- [2] G. Giri *et al.*, *Nature (London)* **480**, 504 (2011).
- [3] L. Friedman, *Phys. Rev.* **133**, A1668 (1964); P. Gosar and S. I. Choi, *ibid.* **150**, 529 (1966); H. Sumi, *J. Chem. Phys.* **70**, 3775 (1979).
- [4] V. M. Kenkre *et al.*, *Phys. Rev. Lett.* **62**, 1165 (1989).
- [5] K. Hannewald *et al.*, *Phys. Rev. B* **69**, 075211 (2004).
- [6] K. Hannewald, V. M. Stojanović, and P. A. Bobbert, *J. Phys.: Condens. Matter* **16**, 2023 (2004).
- [7] Y. C. Cheng and R. J. Silbey, *J. Chem. Phys.* **128**, 114713 (2008).
- [8] J.-D. Picon, M. N. Bussac and L. Zuppiroli, *Phys. Rev. B* **75**, 235106 (2007); V. Stehr *et al.*, *ibid.* **83**, 155208 (2011); C. A. Perroni, V. Marigliano Ramaglia, and V. Cataudella, *ibid.* **84**, 014303 (2011).
- [9] W. Warta and N. Karl, *Phys. Rev. B* **32**, 1172 (1985).
- [10] M. E. Gershenson *et al.*, *Rev. Mod. Phys.* **78**, 973 (2006).
- [11] P. J. Brown *et al.*, *Phys. Rev. B* **63**, 125204 (2001); N. Koch *et al.*, *Phys. Rev. Lett.* **96**, 156803 (2006); R. C. Hatch, D. L. Huber, and H. Höchst, *ibid.* **104**, 047601 (2010); S.-I. Machida *et al.*, *ibid.* **104**, 156401 (2010); J.-F. Chang *et al.*, *ibid.* **107**, 066601 (2011).
- [12] A. Troisi and G. Orlandi, *Phys. Rev. Lett.* **96**, 086601 (2006); A. Troisi, *J. Chem. Phys.* **134**, 034702 (2011).
- [13] S. Fratini and S. Ciuchi, *Phys. Rev. Lett.* **103**, 266601 (2009); S. Ciuchi and S. Fratini, *ibid.* **106**, 166403 (2011).
- [14] V. Coropceanu *et al.*, *Phys. Rev. Lett.* **89**, 275503 (2002).
- [15] A. Girlando *et al.*, *Phys. Rev. B* **82**, 035208 (2010).
- [16] M. Zoli, *Phys. Rev. B* **66**, 012303 (2002); V. M. Stojanović and M. Vanević, *ibid.* **78**, 214301 (2008).
- [17] Y. Li *et al.*, *Phys. Rev. B* **85**, 245201 (2012).
- [18] H. Yoshida and N. Sato, *Phys. Rev. B* **77**, 235205 (2008).
- [19] F. Giustino, S. G. Louie, and M. L. Cohen, *Phys. Rev. B* **76**, 165108 (2007); *Phys. Rev. Lett.* **105**, 265501 (2010); E. Cannuccia and A. Marini, *ibid.* **107**, 255501 (2011).
- [20] P. Giannozzi *et al.*, *J. Phys.: Condens. Matter* **21**, 395502 (2009); S. Baroni *et al.*, <http://www.pwscf.org/>.

- [21] See, e.g., S. Grimme, *J. Comput. Chem.* **27**, 1787 (2006).
- [22] D. Nabok *et al.*, *Phys. Rev. B* **77**, 245316 (2008); C. Ambrosch-Draxl *et al.*, *New J. Phys.* **11**, 125010 (2009).
- [23] S. Baroni *et al.*, *Rev. Mod. Phys.* **73**, 515 (2001).
- [24] J. Noffsinger *et al.*, *Comput. Phys. Comm.* **181**, 2140 (2010).
- [25] I. Souza *et al.*, *Phys. Rev. B* **65**, 035109 (2001); A. A. Mostofi *et al.*, *Comput. Phys. Comm.* **178**, 685 (2008).
- [26] See V. M. Stojanović, N. Vukmirović, and C. Bruder, *Phys. Rev. B* **82**, 165410 (2010), and references therein.
- [27] M. Zoli, *Adv. Cond. Mat. Phys.* **2010**, 815917 (2010).
- [28] A. S. Alexandrov and J. T. Devreese, *Advances in Polarons Physics* (Springer-Verlag, Berlin, 2010).